

# Quantum dimer model with $\mathbb{Z}_2$ liquid ground-state: interpolation between cylinder and disk topologies and toy model for a topological quantum-bit

Grégoire Misguich, Vincent Pasquier

*Service de Physique Théorique, CEA-Saclay, 91191 Gif-sur-Yvette Cédex, France*

Frédéric Mila

*Institut de théorie des phénomènes physiques,  
École Polytechnique Fédérale de Lausanne BSP,  
CH-1015 Lausanne, Switzerland*

Claire Lhuillier

*Laboratoire de Physique Théorique des Liquides  
Université P. et M. Curie and UMR 7600 of CNRS  
Case 121, 4 Place Jussieu, 75252 Paris Cédex, France*

We consider a quantum dimer model (QDM) on the kagome lattice which was introduced recently [Phys. Rev. Lett. **89**, 137202 (2002)]. It realizes a  $\mathbb{Z}_2$  liquid phase and its spectrum was obtained exactly. It displays a topological degeneracy when the lattice has a non-trivial geometry (cylinder, torus, etc). We discuss and solve two extensions of the model where perturbations along lines are introduced: first the introduction of a potential energy term repelling (or attracting) the dimers along a line is added, second a perturbation allowing to create, move or destroy monomers. For each of these perturbations we show that there exists a critical value above which, in the thermodynamic limit, the degeneracy of the ground-state is lifted from 2 (on a cylinder) to 1. In both cases the exact value of the gap between the first two levels is obtained by a mapping to an Ising chain in transverse field. This model provides an example of solvable Hamiltonian for a topological quantum bit where the two perturbations act as a diagonal and a transverse operator in the two-dimensional subspace. We discuss how crossing the transitions may be used in the manipulation of the quantum bit to optimize simultaneously the frequency of operation and the losses due to decoherence.

## I. INTRODUCTION

Quantum dimer models (QDM)<sup>1,2</sup> provide simple examples<sup>3,4</sup> of microscopic Hamiltonians with short-ranged resonating valence-bond ground-states (or dimer liquid) with gapped excitations and no broken symmetry ( $\mathbb{Z}_2$  liquids). It has been known for a long time that such liquids are characterized by topological order:<sup>5</sup> although the system breaks no symmetry and has no local order parameter, the ground-state acquires a degeneracy (in the thermodynamic limit) which depends on the genus of the surface where the model is defined (disk, cylinder, torus, etc.). Remarkably, such a topological degeneracy is insensitive to small local perturbations (such as weak disorder for instance).<sup>6,7,8</sup> On the other hand, it is clear that strong enough local perturbations should lift this degeneracy. Consider for instance a  $\mathbb{Z}_2$  dimer liquid on a cylinder, with a two-fold degenerate ground-state. We turn on an external potential which penalizes (with an energy  $\lambda > 0$ ) any dimer sitting across a line extending from one edge of the cylinder to the other. For very large  $\lambda$ , one effectively “cuts” the cylinder down to a disk topology and one expects a single non-degenerate ground-state. It is therefore natural to expect a phase transition at some intermediate value  $\lambda$ .

We provide here a simple model where the spectrum, and the ground-state degeneracy in particular, can be *exactly* calculated as a function of  $\lambda$  and the system size. This model generalizes a QDM on the kagome lattice

(network of corner-sharing triangles with triangular and hexagonal plaquettes, see Fig. 1)) which was introduced recently.<sup>4</sup> The full spectrum (and wave-functions) can be obtained in an elementary way and excitations consist of static and non-interacting Ising vortices<sup>9</sup> (visons<sup>10</sup>). In this paper we show how the solution of the model extends to a situation where an external potential is applied along a line of the system. The solution is obtained by noting that the bulk of the system decouples from the line and the line is exactly described by an Ising chain in transverse field (ICTF). As a result, we find a finite *critical* value  $\lambda_c$  of the perturbation below which the system behaves as a cylinder (the energy difference between the two quasi-degenerate ground-states is exponentially small in the system size). For  $\lambda > \lambda_c$  the system behaves as a disk and the ground-state is separated from the first excited state by a finite gap  $\mathcal{O}(\lambda - \lambda_c)$ .

It has been argued that gapped systems with a topological degeneracy could provide physical ways to implement quantum-bits (qubits) which would be protected from decoherence by their topological nature.<sup>6,7,11,12</sup> Since no *local* measurement can distinguish the different ground-states if the system is infinitely large, any manipulation (unitary rotation) or measurement (projection) of the state of the qubit through local observables will have to rely on finite-size effects. We discuss this issue in Section V in the light of the present solvable model. The effective Hamiltonian acting on the two lowest levels is expressed in terms of two generators  $T^x$  and  $T^z$  of ro-

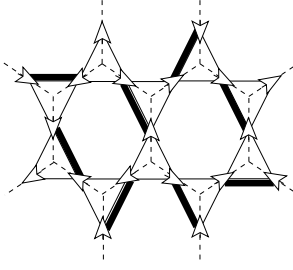


FIG. 1: A dimer covering on the kagome lattice (fat bonds). The corresponding representation with arrows living on the bonds of the hexagonal lattice (dashed lines) is displayed.

tations of the qubit about two quantization axis. We finally explain how one could take advantage of the phase transition at  $\lambda = \lambda_c$  to perform unitary rotations. The problems of this approach, such as thermal excitations, will also be discussed briefly.

## II. ARROW REPRESENTATION, SOLVABLE QDM AND TOPOLOGICAL DEGENERACY

We consider a QDM defined on a kagome lattice with periodic boundary conditions in one direction (cylinder) but the arguments are easily generalized to other topologies.

### A. Arrow representation

Because it is the natural formalism to describe and solve the QDM discussed here, we begin by reminding the representation of dimer coverings of the kagome lattice in terms of *arrows*.<sup>4,13</sup>

The sites of a kagome lattice  $K$  (noted  $i$ ) can be identified with bonds of the hexagonal lattice  $H$ .<sup>19</sup> The triangles of  $K$  (noted  $t$ ) are sites of  $H$ . As for hexagons of  $K$  (noted  $h$ ), they also correspond to hexagons of  $H$ .

From a (fully-packed) dimer covering of  $K$  we orientate the bonds of  $H$  (arrows) in the following way: Each bond of  $H$  is a site of  $K$  which has one dimer, the corresponding arrow points toward the interior of the triangle (of  $K$ ) where the other end of the dimer is. This is illustrated in Fig. 1. As a consequence, the number of incoming arrow(s) is even (0 or 2) at each vertex of  $H$ . Inversely, any arrow configuration satisfying the parity constraint at each vertex defines a unique dimer covering.

We can now define the operators  $\tau^x$ ,  $\tau^z$  and  $\sigma^x$  acting on the arrows. The notations are those of Refs. 4 and 15:

- $\tau_i^z$ : flips the arrow at site  $i \in K$ . Any product  $\tau_i^z \tau_j^z \dots$  around a *close loop* (of  $H$ ) is a “physical” operator in the sense that it conserves all the constraints.

- $\sigma_h^x = \prod_{i=1}^6 \tau_i^z$ . Flips the 6 arrows  $i = 1 \dots 6$  around the hexagon  $h$  (smallest closed loop on  $H$ ).<sup>20</sup> From the definition of  $\tau^z$  above, the  $\sigma^x$  operators satisfy  $(\sigma^x)^2 = 1$  and commute with each other.
- $\tau_i^x$ : Compares the arrow at site  $i$  with the arrow in some (arbitrary) reference covering ( $= +1$  if they are the same,  $-1$  otherwise). The hard-core constraint on dimers translates into  $\tau_0^x \tau_1^x \tau_2^x = 1$  for every triangle (012) of the kagome lattice.

From now on and for most purposes one can forget the dimers themselves and focus only on the bond degrees of freedom  $\tau_i^x = \pm 1$ .<sup>21</sup> We note that, in principle, the  $\tau_i^x = \pm 1$  degrees of freedom could be physically realized with real spins living on a kagome lattice. A strong easy-axis anisotropy could then force them to point toward the center of one of the neighboring triangle.

### B. Bulk Hamiltonian

The QDM introduced in Ref. 4 is

$$\mathcal{H}_0 = - \sum_h \sigma_h^x = - \sum_h \prod_{i=1}^6 \tau_{h_i}^z \quad (1)$$

All the eigenstates are easily obtained because the  $\sigma_h^x$  operators commute with each other and have two eigenvalues  $\sigma_h^x = \pm 1$ .<sup>22</sup>

### C. Topological sectors

As usual for dimer models, the configurations are grouped in topological sectors (TS): two configurations are in the same TS if and only if they can be transformed into each other by a succession of *local*<sup>23</sup> moves. As explained below, there are two TS when the system has the topology of a cylinder.

First draw a cut  $\Delta$  (crossing the bonds of the lattice) going from one edge of the cylinder to the other (Fig. 2). Let  $N_\Delta$  be the number of dimers crossing  $\Delta$ . It has a simple expression in terms of the  $\tau_i^x$ :

$$N_\Delta = \frac{1}{2} \sum_{i=0}^L (1 - \tau_i^x) \quad (2)$$

where the sites  $i = 0 \dots L$  are the centers of the bonds of  $H$  which are cut by  $\Delta$ , as shown in Fig. 3. For simplicity, we assumed in Eq. 2 that no dimer crosses  $\Delta$  in the reference covering.

Any *local* dimer move conserves the parity of  $N_\Delta$  and it is natural to define:

$$T^x = \prod_{i \in \Delta} \tau_i^x = (-1)^{N_\Delta} \quad (3)$$

All coverings with  $T^x = 1$  (resp.  $-1$ ) define a TS, called  $S_+$  (resp.  $S_-$ ) and  $\mathcal{H}_0$  can be diagonalized separately in each sector.

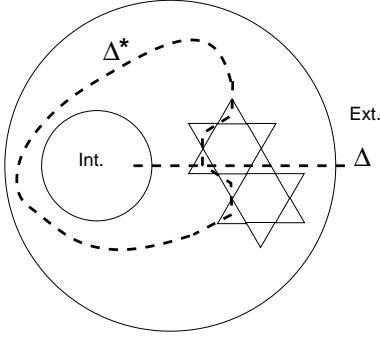


FIG. 2: Kagome lattice on a cylinder with a cut  $\Delta$  going from one edge of the cylinder to the other. The dual cut  $\Delta^*$  passes through the centers of the triangles and winds around the cylinder.

#### D. Topological degeneracy of $\mathcal{H}_0$

It is straightforward to check that  $\mathcal{H}_0$  has the same energy in each sector. Let  $\Delta^*$  be a closed loop encircling the cylinder (Fig. 2) and define an operator

$$T^z = \prod_{i \in \Delta^*} \tau_i^z \quad (4)$$

which flips all the corresponding arrows.  $T^z$  commutes with all the  $\sigma^x$  operators and maps  $S_+$  onto  $S_-$ :

$$T^z T^x = -T^x T^z \quad (5)$$

This shows that if  $|\psi\rangle$  is an eigenstate of  $\mathcal{H}_0$ ,  $T^z|\psi\rangle$  is an eigenstate of  $\mathcal{H}_0$  with the same energy (but in the other TS). This demonstrates the two-fold (topological) degeneracy of the eigenstates of  $\mathcal{H}_0$ .

### III. PERTURBATION LIFTING THE DEGENERACY BETWEEN THE $T^x = \pm 1$ SECTORS

We introduce a potential energy term which couples to the dimers crossing  $\Delta$ :<sup>24</sup>

$$\mathcal{H}_1 = 2\lambda N_\Delta \quad (6)$$

$$= \lambda \sum_{i=0}^L (1 - \tau_i^x) \quad (7)$$

As discussed in the introduction, we expect that a small  $\lambda$  should not affect the two-fold degeneracy while  $\lambda \gg 1$  should leave a single ground-state. In presence of  $\mathcal{H} = \mathcal{H}_0 + \mathcal{H}_1$ ,  $T^x = (-1)^{N_\Delta}$  is still a conserved quantity but  $T^z$  does not commute with  $\mathcal{H}_1$  and the two sectors are no longer degenerate when  $\lambda \neq 0$ . Since for  $\lambda \gg 1$  the system minimizes  $N_\Delta$ , the ground-state of the  $T^x = +1$  sector tends to a state with  $N_\Delta \simeq 0$  and that of the

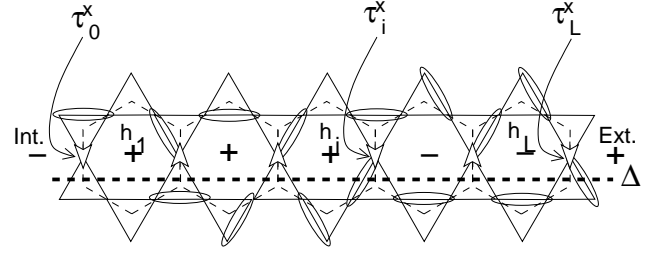


FIG. 3: Dimer covering of the kagome lattice in the vicinity of the cut  $\Delta$  (dashed line). The arrows next to  $\Delta$  (appearing in Eq. 2) are shown. The signs in the hexagons Int.,  $h_1, \dots, h_L$ , Ext. indicate the values of the corresponding pseudospins  $\sigma^z$  (with the assumption that the reference configuration has no dimer crossing  $\Delta$ ).

$T^x = -1$  sector to a state with  $N_\Delta \simeq 1$ . Instead of having a superposition of dimer configurations with different values of  $N_\Delta$  but a fixed *parity* (*non-local* observable), the large  $\lambda$  limit corresponds to a well defined  $N_\Delta$  (sum of *local* operators). While  $T^x$  is still a conserved quantity, we already see that the topological nature of the  $T^x = +1$  and  $T^x = -1$  sectors disappears when  $\lambda$  is large.

The perturbation  $\mathcal{H}_1$  is identical to the one introduced by Ioffe *et al.*<sup>7</sup> in a triangular-lattice QDM in order to manipulate (“phase shifter”) their qubit. However, in our case, *the existence of an arrow representation makes it possible to calculate exactly the spectrum* of  $\mathcal{H} = \mathcal{H}_0 + \mathcal{H}_1$ .

#### A. Mapping to the ICTF

The Hamiltonian  $\mathcal{H} = \mathcal{H}_0 + \mathcal{H}_1$  (Eqs. 1 and 7) can be separated into a “bulk” and a “chain” part as below :

$$\mathcal{H} = \mathcal{H}_\Delta + \mathcal{H}_{\text{bulk}} \quad (8)$$

$$\mathcal{H}_\Delta = - \sum_{i=1}^L \sigma_{h_i}^x + \lambda \sum_{i=0}^L (1 - \tau_i^x) \quad (9)$$

$$\mathcal{H}_{\text{bulk}} = - \sum_{h' \notin \Delta} \sigma_{h'}^x \quad (10)$$

It is important to emphasize that  $\mathcal{H}_\Delta$  and  $\mathcal{H}_{\text{bulk}}$  *commute with each other* and can therefore be treated separately. From now on we concentrate on  $\mathcal{H}_\Delta$ .

*$\sigma^z$  pseudo-spins.*— A  $\sigma_h^z$  operator can be introduced for each hexagon  $h$  in the following way. Due to the local constraint ( $\tau_i^x \tau_j^x \tau_k^x = 1$  on each triangle of  $K$ ), the bonds of  $H$  where  $\tau^x = -1$  necessarily form non-intersecting closed loops.<sup>25</sup> We interpret these loops as domain walls for some Ising pseudo-spins  $\sigma_h^z = \pm 1$  which leave on each hexagon. To remove the two-fold ambiguity we assume that the exterior has a fixed spin  $\sigma_{\text{ext}}^z = 1$ . In turn, this defines a  $\sigma_{\text{int}}^z$  associated to the “interior” (Fig. 4). It is easy to check that this Ising spin labels the TS of the configuration because  $\sigma_{\text{int}}^z = \prod_{i \in \Delta^*} \tau_i^x = T^x$ . The other “bulk” pseudo-spins are those introduced by Zeng

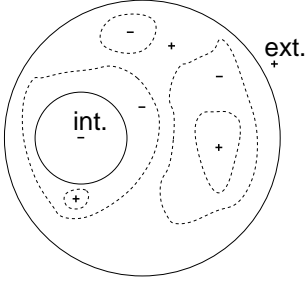


FIG. 4: Cylinder (full lines) and loops (dashed lines) along which a dimer configuration  $c$  differs from the reference. The signs indicate the value of  $\sigma^z$  in each domain.

and Elser.<sup>13</sup> Eventually we mention that  $\sigma_h^z$  and  $\sigma_h^x$  anticommute (they commute if not on the same hexagon), as suggested by the Pauli matrix notation. This is easily checked from the definition of  $\sigma_h^x$  in terms of arrows. From the definition of  $\sigma_h^z$  we have the relation:<sup>4,26</sup>

$$\sigma_h^z \sigma_{h'}^z = \tau_i^x \quad (11)$$

where  $h$  and  $h'$  are the two hexagons touching  $i$ . For an arrow  $i_0$  next to a boundary (say interior), this relation is modified to:

$$\sigma_h^z \sigma_{\text{int}}^z = \tau_{i_0}^x \quad (12)$$

These relations are used to get:

$$\mathcal{H}_\Delta = - \sum_{i=1}^L \sigma_{h_i}^x - \lambda \sum_{i=0}^L \sigma_{h_i}^z \sigma_{h_{i+1}}^z + (L+1)\lambda \quad (13)$$

where the two boundary spins are identified to  $\sigma_0^z = \sigma_{\text{int}}^z$  and  $\sigma_{h_{L+1}}^z = \sigma_{\text{ext}}^z$ . It appears that  $\mathcal{H}_\Delta$  is nothing but the Hamiltonian of an open ICTF with a magnetic exchange  $\lambda$  and a transverse field equal to 1. This model can be solved by a standard Jordan-Wigner transformation and maps onto free fermions. In the thermodynamic limit it has a paramagnetic phase with  $\langle \sigma_h^z \rangle = 0$  for  $|\lambda| < \lambda_c = 1$  and an ordered phase with  $\langle \sigma_h^z \rangle \neq 0$  for  $|\lambda| > \lambda_c = 1$ .

The boundary spins  $\sigma_0^z$  and  $\sigma_{h_{L+1}}^z$  play a special role.  $\sigma_{h_{L+1}}^z = \sigma_{\text{ext}}^z$  is fixed to 1 but  $\sigma_0^z = \sigma_{\text{int}}^z$  is free (but conserved by  $\mathcal{H}_\Delta$ ) and labels the TS. The spectrum of the ICTF can thus be studied separately for  $\sigma_0^z = +1$  or  $\sigma_0^z = -1$ . One takes  $\lambda \geq 0$  (ferromagnetic chain) without loss of generality. The sector with  $\sigma_0^z = +1$  thus corresponds to *unfrustrated boundary conditions* for the (pseudo-spin) chain. On the other hand, choosing  $\sigma_0^z = -1$  amounts to impose at least one Ising domain wall in the system.<sup>27</sup> In the thermodynamic limit both sectors have the same energy *per site* but they may have a finite difference in the total energy (gap). In the paramagnetic phase ( $\lambda < 1$ ), because of the finite spin-spin correlation length  $\xi(\lambda)$ , the frustration has an exponentially small effect on the ground-state energy and the energy difference between the two TS is  $\Delta E \sim \exp(-L/\xi)$  with  $\xi \simeq \ln(1/\lambda)^{-1}$

(see Ref. 12 and Appendix A). On the other hand, in the ferromagnetic phase ( $\lambda > 1$ ), the Ising spins want to order and the boundary condition  $\sigma_0^z \neq \sigma_L^z$  generates a *finite energy* cost  $\Delta E \sim \mathcal{O}(L^0)$  (see Eq. A13).

The result is thus that for  $\lambda < 1$  the ground-state is asymptotically two-fold degenerate in the thermodynamic limit. The gap between the two TS is  $\Delta E \sim \exp(-L/\xi(\lambda))$  where  $\xi$  is the correlation length of the ICTF. In the thermodynamic limit there is a finite critical value  $\lambda_c = 1$  above which the topological degeneracy is destroyed. Above  $\lambda_c$  the Ising pseudo-spins have a positive magnetization. Since  $\sigma_h^z$  is an operator which creates an Ising vortex (vison<sup>4</sup>), it is natural to interpret  $\langle \sigma_h^z \rangle > 0$  as the existence of a *condensate* of those particles (along  $\Delta$ ). This condensation is responsible for changing the “effective” topology of the system from a cylinder into a disk. In this simple model what happens along the chain  $\Delta$  is decoupled from the bulk of the system. The perturbation caused by the potential  $\lambda$  does not extend into the bulk, which remains a liquid with non-interacting and static visons excitations.

#### IV. MIXING THE $T^x = \pm 1$ SECTORS WITH MONOMERS

The perturbation  $\mathcal{H}_1$  discussed in the previous section is not the only way to remove the topological degeneracy. It is well known that in the presence of mobile monomers,  $T^x = (-1)^{N_\Delta}$  is no longer conserved.<sup>28</sup> This property was used in Refs.<sup>7,11</sup> to mix the topological sectors. We will show that in our kagome geometry the arrow representation of the dimer model allows to compute exactly the spectrum of the system when monomers are allowed to be created, to hop and to be destroyed along a line winding around the cylinder. As we will see this model is closely related to that discussed in the previous section:  $\Delta$  is replaced by  $\Delta^*$ , monomers will play the role of the visons and the ICTF will have periodic and antiperiodic boundary conditions instead of open ones.

##### A. Hamiltonian

We relax the parity constraint  $\tau_{t_0}^x \tau_{t_1}^x \tau_{t_2}^x = 1$  on each triangle  $t$  so that triangles with one or three incoming arrows are allowed. When a triangle has *one* incoming arrow, it is naturally interpreted as the presence of a monomer (or hole) at the site of this arrow (see Fig. 5). When a triangle has *three* incoming arrows, we interpret it as a monomer and a dimer which are delocalized over the three sites.<sup>29</sup> Flipping one arrow (*i.e.* acting with  $\tau_i^z$ ) on a dimer state therefore creates two monomers on the nearby triangles (one of which may be delocalized over three sites). We consider the following Hamiltonian:

$$\mathcal{H}'_0 = - \sum_h \sigma_h^x + U \sum_t (1 - \tau_{t_0}^x \tau_{t_1}^x \tau_{t_2}^x) \quad (14)$$

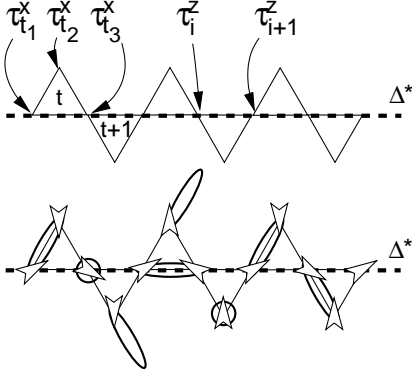


FIG. 5: Top: Kagome lattice in the vicinity of the cut  $\Delta^*$  (dashed line). Bottom: Mixed dimer-monomer configuration and the arrow representation.

$$= - \sum_h \prod_{i=1}^6 \tau_{h_i}^z + U \sum_t (1 - \tau_{t_0}^x \tau_{t_1}^x \tau_{t_2}^x) \quad (15)$$

where  $h_{1...6}$  are the sites around hexagon  $h$  and  $t_{1,2,3}$  the sites of the triangle  $t$  (see Fig. 5).  $U$  is a large energy enforcing the constraint on low-energy states. This type of model was first considered by Kitaev.<sup>6</sup> For  $U > 0$  the ground-state of the Hamiltonian Eq. 15 is the same as for  $U = \infty$  (equivalent to Eq. 1) since  $\tau_{t_0}^x \tau_{t_1}^x \tau_{t_2}^x$  commutes with all the  $\sigma^x$ . However, static pairs of monomers are present in excited states with energies greater than  $2U$  above the ground-state.

As Ioffe *et al.*,<sup>7,11</sup> we wish to use these monomers to couple the two TS. For this purpose the monomers are allowed to be created and to propagate along one closed loop  $\Delta^*$  winding around the cylinder (Fig. 2). The simplest term which does this is

$$\mathcal{H}'_1 = -\mu U \sum_{i \in \Delta^*} \tau_i^z \quad (16)$$

(this choice of normalization will make the analogy with the  $\lambda$  perturbation clearer). When a  $\tau_i^z$  term acts on a site located between two triangles satisfying the constraint ( $\tau_{t_0}^x \tau_{t_1}^x \tau_{t_2}^x = 1$ ), it creates a pair of monomers. When it acts on a pair of triangles violating the constraint, the pair of monomers is destroyed. If it acts on a site located between triangles with different values of  $\tau_{t_0}^x \tau_{t_1}^x \tau_{t_2}^x$ , a monomer hops from one triangle to the other.

### B. Mapping to the ICTF

As in Eq. 8,  $\mathcal{H}'_0 + \mathcal{H}'_1$  splits into a bulk and a one-dimensional parts:<sup>30</sup>

$$\mathcal{H}'_0 + \mathcal{H}'_1 = \mathcal{H}'_{\text{bulk}} + \mathcal{H}_{\Delta^*} \quad (17)$$

$$\mathcal{H}'_{\text{bulk}} = - \sum_h \sigma_h^x + U \sum_{t \notin \Delta^*} (1 - \tau_{t_0}^x \tau_{t_1}^x \tau_{t_2}^x) \quad (18)$$

$$\mathcal{H}_{\Delta^*} = -\mu U \sum_{i \in \Delta^*} \tau_i^z + U \sum_{t \in \Delta^*} (1 - \tau_{t_0}^x \tau_{t_1}^x \tau_{t_2}^x) \quad (19)$$

One can simply check that  $\mathcal{H}_{\Delta^*}$  and  $\mathcal{H}'_{\text{bulk}}$  commute with each other so that one has to study a one-dimensional model  $\mathcal{H}_{\Delta^*}$ . This model is identical to a closed ICTF (with periodic or antiperiodic boundary conditions) as explained below. Each *triangle*  $t$  crossed by  $\Delta^*$  corresponds to a *site* of the spin chain. The associated transverse-field term for this Ising spin is:

$$\tilde{\sigma}_t^x = \tau_{t_0}^x \tau_{t_1}^x \tau_{t_2}^x \quad (20)$$

We define the  $z$  component of the spins as

$$\tilde{\sigma}_t^z = \tau_0^z \tau_1^z \cdots \tau_{i(t)}^z \quad (21)$$

where 0 is an (arbitrary) origin on  $\Delta^*$  and  $i(t)$  is the site of  $K$  in common with triangles  $t$  and  $t-1$ . It is simple to check that the  $\tilde{\sigma}^x$  and  $\tilde{\sigma}^z$  defined above (not to be confused with  $\sigma^x$  and  $\sigma^z$ ) obey the usual Pauli matrix algebra and play the role of spin- $\frac{1}{2}$  operators. In addition, these definitions insure that

$$\tilde{\sigma}_t^z \tilde{\sigma}_{t+1}^z = \tau_{t_3}^z \quad (22)$$

where  $t_3$  is the common site between triangles  $t$  and  $t+1$  (as in Fig. 5). Because  $\Delta^*$  is a closed curve, a special care is needed for the last term:

$$T^z \tilde{\sigma}_{L-1}^z \tilde{\sigma}_0^z = \tau_0^z \quad (23)$$

where  $T^z$  (defined in Eq. 4) commutes with  $\mathcal{H}_{\Delta^*}$  (in the same way we had before  $[\mathcal{H}_{\Delta}, T^x] = 0$ ). It can be successively set to  $\pm 1$  to obtain the whole spectrum. With these notations  $\mathcal{H}_{\Delta^*}$  reads

$$\begin{aligned} \frac{1}{U} \mathcal{H}_{\Delta^*} = & -\mu \left( T^z \sigma_{L-1}^z \tilde{\sigma}_0^z + \sum_{t=0}^{L-2} \tilde{\sigma}_t^z \tilde{\sigma}_{t+1}^z \right) \\ & - \sum_{t=0}^{L-1} \tilde{\sigma}_t^x + \text{cst.} \end{aligned} \quad (24)$$

This is the Hamiltonian of an ICTF with periodic boundary conditions when  $T^z = 1$  and antiperiodic boundary conditions when  $T^z = -1$ . As for  $\mathcal{H}_{\Delta}$ , the model has, in the thermodynamic limit, a phase transition at  $\mu_c = 1$  between a paramagnetic phase and a ferromagnetic phase. The calculation of the gap between the two sectors amounts to study a closed ICTF with periodic and antiperiodic boundary conditions. The exact result for the energy difference  $\Delta E'$  is derived in the Appendix B (see also Ref. 12) with the help of a Jordan-Wigner transformation. In the limit of a large system ( $L \gg 1$ ) it is given by

$$\begin{aligned} \Delta E' &= E_+ - E_- \\ &\simeq 2U \sqrt{\frac{1-\mu^2}{L\pi}} \mu^L \text{ for } \mu < 1 \end{aligned} \quad (25)$$

$$\simeq 2U(\mu-1) \text{ for } \mu > 1 \quad (26)$$

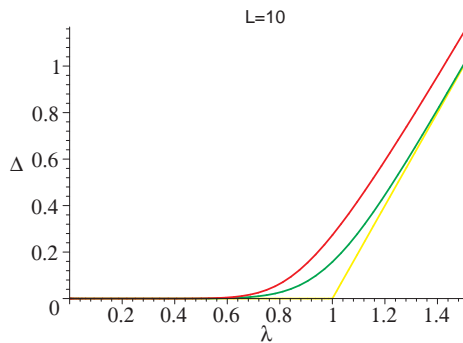


FIG. 6: Effect of a change of boundary conditions on the ground-state energy of an ICTF with  $N = 10$  spins as a function of the (ferromagnetic) exchange  $\lambda$ . Circles: closed chain with periodic and anti-periodic boundary conditions. Thin line: Ground-state energy difference between open chain with ferromagnetic ( $\uparrow \dots \uparrow$ ) and antiferromagnetic ( $\downarrow \dots \uparrow$ ) boundary conditions. Thick line:  $N = \infty$  case (same result for the open and closed chains).

The result for  $L = 10$  is plotted in Fig. 6. As for  $\mathcal{H}_\Delta$ , the critical value  $\mu_c = 1$  separates a regime with an exponentially small splitting between the sectors (Eq. 25) and a regime with a finite gap between them (Eq. 26). In the spin language, the ferromagnetic phase is characterized by  $\langle \tilde{\sigma}^z \rangle \neq 0$ . Going back to dimer/monomers variables, we find that  $\tilde{\sigma}_t^z$  flips all the arrows located on  $\Delta^*$  between the origin and  $t$ . Thus, it creates or annihilates a pair of monomers sitting at both ends of the string or move a monomer from one end to the other. In both cases  $\tilde{\sigma}_t^z$  creates or destroys a monomer on the triangle  $t$ .<sup>31</sup>  $\langle \tilde{\sigma}^z \rangle \neq 0$  can thus be interpreted as a *condensation* of monomers along  $\Delta^*$ . This is equivalent to the condensate of visons mentioned in the case of  $\mathcal{H}_\Delta$  when  $\lambda > 1$ .

To conclude this section we discuss a difference between the  $\lambda$  and the  $\mu$  perturbations. In the limit where  $\lambda \rightarrow \infty$  no dimer can sit on  $\Delta$  anymore and the torus is reduced to a rectangle, as if the lattice had been cut with scissors. If the same geometrical picture was true for the perturbation  $\mu$  along  $\Delta^*$ , one would erroneously conclude that the system is effectively transformed into *two* cylinders with a  $2 \times 2 = 4$ -fold ground-state degeneracy. This is incorrect for the following reason. The path  $\Delta^*$  chosen to define  $T^z(\Delta^*)$  (Eq. 4) may be shifted by multiplication with a  $\sigma^x$  operator:

$$\sigma^x(h)T^z(\Delta_1^*) = T^z(\Delta_2^*) \quad (27)$$

where  $h$  is a hexagon next to  $\Delta_1^*$  and  $\Delta_2^*$  is identical to  $\Delta_1^*$  except that it passes on the other side of  $h$ . From Eq. 27, we see that  $T^z(\Delta_1^*)|0\rangle$  does not depend on the location of  $\Delta_1^*$  as long as this closed curve is deformed by passing only on hexagons with  $\sigma^x(h) = 1$ . In the case of a the perturbation  $\mu$ , the ground-state satisfies  $\sigma^x(h)|0\rangle = |0\rangle$  for all hexagons  $h$ , even those along  $\Delta^*$  (this is not true for the  $\lambda$  perturbation which does not commute with  $\sigma^x$ ). Therefore one cannot independently

flip the topological sector of the “upper” cylinder with some  $T_1^z$  without changing the sector of the “lower part” which is controlled by a  $T_2^z$ , since  $T_1^z|0\rangle = T_2^z|0\rangle$ .

## V. A TOY MODEL FOR A TOPOLOGICAL QUBIT

Kitaev<sup>6</sup> suggested that systems with topologically degenerate ground-states could be used to realize qubits protected from decoherence. This suggestion was then made more precise by Ioffe *et al.*<sup>7,11</sup> and Douçot *et al.*<sup>12,18</sup> who proposed to use Josephson junctions arrays to implement such a system. As mentioned in the introduction, the topological nature of the degeneracy makes it difficult to “manipulate” (perform unitary rotation) because it is almost insensitive to local couplings. On the other hand, it may be difficult to apply a perturbation corresponding to a non-local operator (such as  $T^z$  or  $T^y$ ). If however the system allows for an hardware implementation of such a non-local operator,<sup>32</sup> it represents a dangerous channel through which perturbations could bypass the topological protection and contribute to decoherence of the qubit. If such a non-local coupling to the system exists, one must be able to “disconnect” it efficiently when it is not active.

The clever solution proposed in Ref. 7,11 consists in perturbing the system by two external potentials acting along two lines, exactly as  $\Delta$  and  $\Delta^*$ . While these perturbations are local (more precisely they are sums of local terms), they induce a splitting of the two ground-states proportional to  $\lambda^L$  and therefore induce a slow precession of the qubit. In this section we take advantage of the exact solution of the model to discuss these effects beyond the regime where  $\lambda^L \ll 1$ .

### A. Unitary rotations

Combining the perturbations along  $\Delta$  and  $\Delta^*$  the Hamiltonian is

$$\mathcal{H}(\lambda, \mu) = \mathcal{H}_{0'} + \mathcal{H}_{1'} + \mathcal{H}_1 \quad (28)$$

$$= - \sum_h \prod_{i=1}^6 \tau_{h_i}^z + U \sum_t (1 - \tau_0^x \tau_1^x \tau_2^x) - \mu U \sum_{i \in \Delta^*} \tau_i^z - \lambda \sum_{i \in \Delta} (\tau_i^x - 1) \quad (29)$$

From the previous calculations we know that  $\mathcal{H}(\lambda, \mu = 0)$  lifts the degeneracy of the two TS. It acts in this two-dimensional subspace as  $\Delta E(\lambda)T^x$ , where  $\Delta E(\lambda)$ , given in Eqs. A13 and A15, is the energy difference between ferromagnetic and antiferromagnetic boundary conditions for an ICTF with exchange  $\lambda$  (and a unit transverse field). On the other hand,  $\mathcal{H}(\lambda = 0, \mu)$  mixes the two sectors. Its action is described by  $U \Delta E'(\mu)T^z$  where  $\Delta E'$  (Eq. B23) is energy difference between periodic and

antiperiodic boundary conditions for an ICTF (with exchange  $\mu U$  and transverse field  $U$ ).<sup>33</sup>

If the system is operated below the critical values of  $\lambda$  and  $\mu$ , the qubit precesses at a frequency which is exponentially small in the system size. The cylinder topology and the low density of monomers protect the degeneracy of the spectrum. This is the regime mentioned by Ioffe *et al.*. However, the system size cannot be too large because the time required for a unitary rotation would become exponentially long. On the other hand, if the system is not large enough, its topology does not fully protect it from decoherence by external perturbations.

If one of the external parameters ( $\lambda$  or  $\mu$ ) is pushed above its critical value, the frequency becomes finite, even in case of large system size. We may therefore take advantage of the phase transitions in a large system. In such a case the qubit is topologically protected as long as  $\lambda$  and  $\mu$  are smaller than their critical values, even if they are not precisely set to zero or if they introduce some noise. It is only during the “manipulation” ( $\lambda(t) > 1$  or  $\mu(t) > 1$ ) that the state of the qubit evolves (and is sensitive to the external noise entering through  $\Delta$  or  $\Delta^*$ ).

To preserve an adiabatic evolution one must avoid transitions to other eigenstates. However the gap in the spectrum of the ICTF becomes small (of the order of  $\sim 1/L$ ) in the vicinity of the transition. This limits the typical time of the unitary rotation to be at least of the order of  $L$ . This *linear* dependence in the system size is an interesting property because it should be compared to the *exponential* dependence ( $\sim \lambda^{-L}$ ) present in the perturbative regime. Also because of this small gap, the temperature must be  $T \ll 1/L$  to avoid thermal excitations when  $\lambda$  (or  $\mu$ ) is close to 1. Using the transition to perform unitary rotation therefore seems to improve the time of operation and could enable to use a larger system and to benefit from a stronger topological protection. It also requires to work at lower temperature than for a qubit operated in the perturbative ( $\lambda, \mu \ll 1$ ) regime only and this may represent a severe limitation.

## B. Reading out the state of the qubit

We assume that the qubit is in a linear combination of the two topological sectors:  $|\psi\rangle = \alpha|+\rangle + \beta|-\rangle$  where  $T^x|+\rangle = |+\rangle$  and  $T^x|-\rangle = -|-\rangle$ . We wish to measure  $|\alpha|^2$  with a *local* observable. This is not directly possible if the system is very large since any local observable has expectation values in  $|+\rangle$  and  $|-\rangle$  which are exponentially close. Likewise, a local observable has a vanishing matrix element between  $|+\rangle$  and  $|-\rangle$ . A possible procedure could be to switch adiabatically the potential  $\lambda$  above the transition. For a strong enough  $\lambda$ , the state  $|+\rangle$  evolves to a superposition of dimer coverings with no dimer crossing  $\Delta$ . On the other hand,  $|-\rangle$  evolves to a superposition of dimer coverings with *one* dimer crossing  $\Delta$ . This is because the parity ( $T^x$ ) is a conserved quantity under the evolution but the ground-state has to minimize  $N_\Delta$

as  $\lambda(t)$  grows. A (projective) measurement detecting the presence of a dimer on some bond crossing  $\Delta$  will thus give 1 with probability  $|\alpha|^2/L$ . The whole operation has to be repeated a large number of times ( $\sim L$ ) before  $|\alpha|^2$  is known with a reasonable accuracy but one may improve the efficiency of the measurement by having a bond along  $\Delta$  where the energy cost of a dimer is less than on other bonds (in which case the dimer, if present, will localize on this particular bond when  $\lambda$  becomes large). Of course the reading procedure described above suffers from the same limitations (time proportional to  $L$  and low temperature) as the unitary rotation.

## VI. CONCLUSIONS

We have shown that the QDM of Eq. 1 can be simply solved in the presence of two kinds of perturbations: an external potential that couples to dimers crossing a line or the inclusion of monomers. This provides a simple example of system with a  $\mathbb{Z}_2$  fractionalized phase where the topological degeneracy is destroyed by tuning an external parameter through a quantum phase transition (belonging to the classical Ising 2D universality class).

We also discussed some properties of this toy model from the point of view of an ideal topological qubit, in which case the exact solution allows to follow the two lowest eigenstates as a function of some external parameters. These two parameters can be used to perform unitary rotations of the qubit and provide an exactly solvable version of some ideas introduced previously.<sup>7</sup> In addition, we pointed out that the phase transition could, in principle, be used to improve the robustness to decoherence because it could enable to use a larger (although not infinite) system. Concerning the measurement of the qubit, we also emphasize the interesting properties of the phase transition as it turns a non-local property (*parity* of the number of dimers crossing a line) into a local property (*dimer density*). From this point of view, we note that the method has some resemblance with the flux trapping experiment imagined by Senthil and Fisher<sup>10</sup> to detect visons in a  $\mathbb{Z}_2$  fractionalized systems.

## Acknowledgments

We thank Benoît Douçot for stimulating discussions and D. Ivanov for useful comments on the manuscript. G. M. is in part supported by the Ministère de la Recherche et des Nouvelles Technologies with an ACI grant and acknowledges the hospitality of IRRMA.

## APPENDIX A: GROUND-STATE ENERGY OF AN ICTF WITH OPEN BOUNDARY CONDITIONS

We apply fixed boundary conditions to an open ICTF and compute the energy difference between the case of ferromagnetic boundary conditions (two fixed up spins at the ends) and antiferromagnetic boundary conditions (one up spin at one end and a down spin at the other). This result has been obtained recently by Douçot *et al.*<sup>12</sup> but we give here for completeness a detailed derivation of the result.

### 1. Hamiltonian and free fermions

The Hamiltonian is

$$\mathcal{H} = - \sum_{n=1}^L \sigma_n^x - \mu \sum_{n=0}^L \sigma_n^z \sigma_{n+1}^z \quad (\text{A1})$$

with two fixed spins at the ends of the chain:  $\sigma_{L+1}^z = 1$  and  $\sigma_0^z = \pm 1$  depending on the boundary conditions. Using a standard Jordan-Wigner transformation to represent the Ising operators with spinless fermions:

$$\sigma_n^x = 2c_n^\dagger c_n - 1 \quad (\text{A2})$$

$$\sigma^y + i\sigma^z = 2c_n^\dagger \exp\left(i\pi \sum_{i=0}^{n-1} c_i^\dagger c_i\right) \quad (\text{A3})$$

$$\sigma_n^z \sigma_{n+1}^z = (c_n^\dagger + c_n)(c_{n+1} - c_{n+1}^\dagger) \quad (\text{A4})$$

$\mathcal{H}$  is quadratic in the fermion operators and can be diagonalized by a Bogoliubov transformation. To find the quasi-particle creation operators  $d^\dagger$  we consider the following form (Ansatz):<sup>34</sup>

$$d_\omega^\dagger = f_\omega^\dagger - f_{\omega-1}^\dagger \quad (\text{A5})$$

$$f_\omega^\dagger = \sum_{n=0}^{L+1} \omega^n (c_n^\dagger + c_n) + ib(\omega) \sum_{n=0}^{L+1} \omega^n (c_n^\dagger - c_n) \quad (\text{A6})$$

where  $\omega$  and  $b(\omega)$  have to be determined. One can check that

$$[\mathcal{H}, d_\omega^\dagger] = E(\omega) d_\omega^\dagger \quad (\text{A7})$$

$$[\mathcal{H}, d_\omega] = -E(\omega) d_\omega$$

with  $E(\omega) \geq 0$

provided the following equations are satisfied:

$$E(\omega) = -2ib(\omega)(1 + \lambda\omega^{-1}) \quad (\text{A8})$$

$$iE(\omega)b(\omega) = -2(1 + \lambda\omega) \quad (\text{A9})$$

$$\omega^{L+1} - \omega^{-L-1} = -\lambda(\omega^{L+2} - \omega^{-L-2}) \quad (\text{A10})$$

The two first equations come from the terms  $0 \leq n \leq L$  in Eq. A7. These equations determine the energy of the quasi-particles as a function of  $\omega$ :

$$E(\omega) = 2\sqrt{\lambda^2 + \lambda(\omega + \omega^{-1}) + 1} \quad (\text{A11})$$

The third equation (A10) comes from the boundary at  $n = L + 1$  and is a constraint on the available  $\omega$ .

### 2. Case $\lambda \geq \frac{L+1}{L+2}$

For  $\lambda \geq \frac{L+1}{L+2}$  the Eq. A10 has  $L + 1$  distinct solutions of the form:

$$\begin{aligned} \omega &= e^{ik} \text{ with } k \in ]0, \pi] \\ \lambda &= -\frac{\sin((L+1)k)}{\sin((L+2)k)} \end{aligned} \quad (\text{A12})$$

These fermionic levels are those required to describe the  $L + 1$  spins  $n = 0 \cdots L$ . Because we have chosen  $E$  to be always positive, the absolute ground-state (whatever  $\sigma_0^z$ ) is the vacuum  $|0\rangle$  of the  $d_\omega^\dagger$ . The lowest excited state is  $d_{k_0}^\dagger |0\rangle$  where we have added the fermion with the smallest energy  $\Delta$ . It corresponds to the solution  $k_0$  of Eq. A12 which is the closest to  $\pi$ . This solution can be calculated by an expansion in  $1/L$  and we obtain

$$\Delta = 2(\lambda - 1) + \frac{\lambda\pi^2}{(\lambda - 1)L^2} + \mathcal{O}(L^{-3}) \quad (\text{A13})$$

So far we have not specified the value of  $\sigma_0^z$  corresponding to each level. In the limit where  $\lambda \gg 1$  it is clear that the ground-state is in the sector  $\sigma_0^z = 1$ . Since one can show that no level-crossing occur for  $\lambda > 0$  in such a finite chain, the fermion vacuum  $|0\rangle$  satisfies  $\sigma_0^z |0\rangle = |0\rangle$  for all  $\lambda > 0$  and correspond to a state of the system with ferromagnetic boundaries. On the other hand, inserting any  $d_\omega^\dagger$  fermion changes the sign of  $\sigma_0^z$  (since all the  $d_\omega^\dagger$  anticommute with  $\sigma_0^z = c_0^\dagger + c_0$ ). The first excited state  $d_{k_0}^\dagger |0\rangle$  is thus the ground-state of the system with antiferromagnetic boundary conditions ( $\sigma_0^z = -1$ ) and the gap between the two sectors is given by  $\Delta$  (Eq. A13).

### 3. Case $0 < \lambda \leq \frac{L+1}{L+2}$

In the range  $0 > \lambda \geq \frac{L+1}{L+2}$ , only  $L$  solutions of the form Eqs. A12 exist. The “missing” solution  $\omega_0$  has the lowest energy and is real:  $\omega_0 \in ]-\infty, 0]$ . It corresponds to a bound-state (imaginary wave-vector) for the fermions. In the thermodynamic limit one has  $\omega_0 = -\frac{1}{L}$  and finite-size corrections can be evaluated:

$$\omega_0 = -\frac{1}{L} + \lambda^{2L+1} (1 - \lambda^2) + \mathcal{O}(L\lambda^{4L}) \quad (\text{A14})$$

which gives an energy gap

$$\Delta = 2\lambda^{L+1} (1 - \lambda^2) + \mathcal{O}(L\lambda^{3L}) \quad (\text{A15})$$

As before, this gap is the ground-state energy difference between antiferromagnetic and ferromagnetic boundary conditions for the spin chain.



## APPENDIX B: GROUND-STATE ENERGY OF AN ICTF WITH PERIODIC OR ANTIPERIODIC BOUNDARY CONDITIONS

We compute the ground-state energy of a closed ICTF with periodic and anti-periodic boundary conditions. The latter result has also been obtained recently by Douçot *et al.*<sup>12</sup> but we give here a detailed derivation of the result. We also note that this calculation has some similarities with the evaluation of the ground-state energy splitting in the triangular lattice QDM at the Rokhsar Kivelson point (using a Pfaffian technique).<sup>8</sup>

### 1. Periodic boundary conditions

The Hamiltonian is :

$$\mathcal{H} = - \sum_{n=0}^{L-1} \sigma_n^x - \mu \sum_{n=0}^{L-1} \sigma_n^z \sigma_{n+1}^z \quad (\text{B1})$$

with  $\sigma_L^z = \sigma_0^z$ . The Ising operators are represented with spinless fermions as in Eqs. A2, A3 and A4. Due to the periodic boundary conditions we have also

$$\begin{aligned} \sigma_{L-1}^z \sigma_0^z &= -(c_{L-1}^\dagger + c_{L-1})(c_0 - c_0^\dagger) \\ &\times \exp \left( i\pi \sum_{n=0}^{L-1} c_n^\dagger c_n \right) \end{aligned} \quad (\text{B2})$$

It is simple to check that

$$\prod_{n=0}^{L-1} \sigma_n^x = \exp \left( i\pi \sum_{n=0}^{L-1} c_i^\dagger c_i \right) \quad (\text{B3})$$

is a conserved quantity. The spectrum can thus be studied separately in the sectors  $\prod_{n=0}^{L-1} \sigma_n^x = \pm 1$ . However  $\mathcal{H}$  has off-diagonal matrix element in the natural Ising basis which are all  $\leq 0$ . This insures that the ground-state has only positive weight in this basis and it therefore belongs to sector

$$\prod_{n=0}^{L-1} \sigma_n^x = 1 \quad (\text{B4})$$

In the following we thus consider fermions subjected to *anti-periodic boundary conditions* (see Eqs. B3 and B4 and the  $-$  sign in the r.h.s of Eq. B2).

After Fourier transform the Hamiltonian becomes:

$$\begin{aligned} \mathcal{H}_{\text{chain}} &= \sum_{k=\frac{2n+1}{L}\pi} \left[ \left( i\mu \sin(k) c_k^\dagger c_{-k}^\dagger + \text{H.c} \right) \right. \\ &\quad \left. - 2c_k^\dagger c_k (\mu \cos(k) + 1) + 1 \right] \end{aligned} \quad (\text{B5})$$

which is diagonalized by a Bogoliubov transformation

$$\mathcal{H}_{\text{chain}} = \sum_{k=\frac{2n+1}{L}\pi} \epsilon(k) \left[ d_k^\dagger d_k - \frac{1}{2} \right] \quad (\text{B6})$$

$$\epsilon(k) = 2\sqrt{\mu^2 + 1 + 2\mu \cos(k)} \quad (\text{B7})$$

Using the explicit form of the transformation and the anti-periodic boundary conditions on the fermions, one can show that the vacuum  $|0\rangle$  of the  $d_k^\dagger$  fermions satisfies:

$$\exp \left( i\pi \sum_{n=0}^{L-1} c_n^\dagger c_n \right) |0\rangle = +|0\rangle \quad (\text{B8})$$

This is consistent with Eq. B4 and the ground state is thus  $|0\rangle$ . Its energy is

$$E_P = -\frac{1}{2} \sum_{k=\frac{2n+1}{L}\pi} \epsilon(k) \quad (\text{B9})$$

### 2. Anti-periodic boundary conditions

To insure that  $\sigma_L^z = -\sigma_0^z$ , the fermions are now subjected to *periodic* boundary conditions (see Eq. B2). However, for  $\mu > 1$  it is necessary to add one  $d_k^\dagger$  fermion to insure the correct parity under a global spin flip. Since the dispersion relation  $\epsilon(k)$  is minimum in  $\epsilon(k=0) = 2|\mu-1|$  the ground-state for  $\mu > 1$  is

$$|1\rangle = d_0^\dagger |0\rangle \quad (\text{B10})$$

The ground-state energy of the chain with anti-periodic boundary conditions is thus

$$E_A = -\frac{1}{2} \sum_{k=\frac{2n}{L}\pi} \epsilon(k) + 2(\mu-1) \text{ for } \mu > 1 \quad (\text{B11})$$

$$= -\frac{1}{2} \sum_{k=\frac{2n}{L}\pi} \epsilon(k) \text{ for } 0 \leq \mu \leq 1 \quad (\text{B12})$$

### 3. Energy difference

From the calculation above the energy difference between the ground-states of the two boundary conditions is (for  $\mu \leq 1$ ) :

$$\begin{aligned} E_A - E_P &= \sqrt{2\mu} \sum_{n=0}^{L-1} \left[ \sqrt{\cosh \alpha_0 - \cos(k_{n+\frac{1}{2}})} \right. \\ &\quad \left. - \sqrt{\cosh \alpha_0 - \cos(k_n)} \right] \end{aligned} \quad (\text{B13})$$

where

$$k_n = \frac{2n\pi}{L} \quad (\text{B14})$$

and  $\alpha_0$  is defined by

$$\cosh \alpha_0 = \frac{\mu^2 + 1}{2\mu} \quad (\geq 1) \quad (\text{B15})$$

$$\alpha_0 = -\ln(\mu) \quad (\text{B16})$$

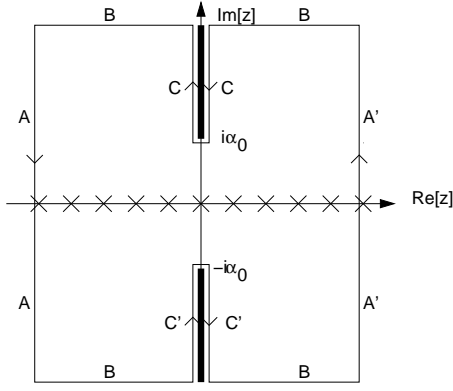


FIG. 7: Contour in the complex plane used to define the integral  $I_C$ . The crosses on the real axis indicate the poles of  $1/\sin(Lz)$  and the fat segments on the imaginary axis indicate the branch cuts of  $f(z)$ . The region B is sent to  $\text{Im}[z] = \pm\infty$ .

The difference between the two sums can be related to a contour integral  $I_0$  in the complex plane:

$$E_A - E_P = \sqrt{2\mu} L I_0 \quad (\text{B17})$$

where

$$I_0 = -\frac{1}{2i\pi} \oint_C \frac{f(z)}{\sin(Lz)} dz \quad (\text{B18})$$

and

$$f(z) = \sqrt{\cosh \alpha_0 - \cos(z)} \quad (\text{B19})$$

The contour is shown Fig. 7. The equality Eq. B17 can be demonstrated by using the fact that the poles inside the contour are located at  $z = k_n$  and  $z = k_{n+\frac{1}{2}}$  and have alternating residues proportional to  $-f(k_n)/L$  and  $+f(k_{n+\frac{1}{2}})/L$ . The contour can be decomposed into several regions:  $I_0 = I_A + I_{A'} + I_B + I_C + I_{C'}$  (Fig. 7). Using the odd parity of the integrand under  $z \rightarrow -z$  one has

$I_C = I_{C'}$  and using the periodicity under  $z \rightarrow z + 2\pi$  one finds  $I_A + I_{A'} = 0$ . The integrand is exponentially small when  $\text{Im}[z] \rightarrow \pm\infty$  so the region B does not contribute. We therefore have  $I_0 = 2I_C$ . The integral over the region C is given by the discontinuity of the integrand along the branch cut:

$$\begin{aligned} I_C &= \frac{1}{2i\pi} \int_{\alpha_0}^{\infty} i dr \left[ \frac{f(ir + o^-)}{\sin(L(ir + o^-))} - \frac{f(ir + o^+)}{\sin(L(ir + o^+))} \right] \\ &= \frac{1}{\pi} \int_{\alpha_0}^{\infty} dr \frac{\sqrt{\cosh(r) - \cosh(\alpha_0)}}{\sinh(Lr)} \end{aligned} \quad (\text{B20})$$

When the system size is large ( $L \rightarrow \infty$ ) the behavior of  $I_C$  is dominated by values of  $r$  close to  $\alpha_0$ . In this limit

$$\begin{aligned} I_C &\simeq \frac{\sqrt{\sinh \alpha_0}}{\pi} \int_{\alpha_0}^{\infty} dr e^{-Lr} \sqrt{r - \alpha_0} \\ &\simeq \frac{\sqrt{\sinh \alpha_0}}{2\sqrt{\pi}} e^{-L\alpha_0} L^{-\frac{3}{2}} \end{aligned} \quad (\text{B21})$$

so that the energy difference is

$$\begin{aligned} E_A - E_P &= 2\sqrt{2\mu} L I_C \\ &\simeq 2\sqrt{\frac{2\mu \sinh \alpha_0}{L\pi}} e^{-L\alpha_0} \end{aligned} \quad (\text{B22})$$

$$\simeq 2\sqrt{\frac{1 - \mu^2}{L\pi}} \mu^L \quad (\text{B23})$$

The calculation of  $E_A - E_P$  for  $\mu > 1$  is almost identical to the  $\mu < 1$  case described above. The difference between the sums of  $\epsilon(k)$  on 'even' and 'odd' momenta is again expressed with the integral  $I_C$  but with  $\alpha_0 = \ln(\mu)$ . Combining this with Eqs. B9 and B11 gives:

$$E_A - E_P = 2(\mu - 1) + 2\sqrt{\frac{\mu^2 - 1}{L\pi}} \mu^{-L} \quad (\text{B24})$$

<sup>1</sup> D. S. Rokhsar and S. A. Kivelson, Phys. Rev. Lett. **61**, 2376 (1988).

<sup>2</sup> The configurations of a *classical* dimer model are subsets of lattice bonds in which every site is taken once. In other words, every site is occupied by exactly one dimer. In a *quantum* dimer model, these configurations form an orthonormal basis of the Hilbert space. The Hamiltonian generally has dimer hopping terms (kinetic energy) which allow  $n \geq 2$  dimers to hop on empty bonds around closed loops of length  $2n$ . The Hamiltonian may also include diagonal (potential) terms which favor or penalize some particular local patterns. For a brief introduction to QDM, see for instance the section 5 of G. Misguich and C. Lhuillier. Review chapter in the book "Frustrated spin systems", edited by H. T. Diep, World-Scientific (2005). [cond-mat/0310405]

<sup>3</sup> R. Moessner and S. L. Sondhi, Phys. Rev. Lett. **86**, 1881 (2001).

<sup>4</sup> G. Misguich, D. Serban, V. Pasquier, Phys. Rev. Lett. **89**, 137202 (2002).

<sup>5</sup> X.G. Wen, Phys. Rev. B **44**, 2664 (1991).

<sup>6</sup> A. Yu. Kitaev, Annals Phys. **303**, 2 (2003). [quant-ph/9707021].

<sup>7</sup> L. B. Ioffe, M. V. Feigel'man, A. Ioselevich, D. Ivanov, M. Troyer and G. Blatter, Nature **415**, 503 (2002).

<sup>8</sup> A. Ioselevich, D. A. Ivanov and M. V. Feigelman, Phys. Rev. B **66**, 174405 (2002).

<sup>9</sup> N. Read and B. Chakraborty, Phys. Rev. B **40**, 7133 (1989), S. Kivelson, Phys. Rev. B **39**, 259 (1989).

<sup>10</sup> T. Senthil and M. P. A. Fisher, Phys. Rev. Lett. **86**, 292 (2001); Phys. Rev. B **63**, 134521 (2001).

- <sup>11</sup> L. B. Ioffe and M. V. Feigel'man, Phys. Rev. B **66**, 224503 (2002)
- <sup>12</sup> B. Douçot, M. V. Feigel'man, L. B. Ioffe, and A. S. Ioselevich, cond-mat/0403712.
- <sup>13</sup> V. Elser and C. Zeng. Phys. Rev. B **48**, 13647 (1993).
- <sup>14</sup> See section III of G. Misguich, D. Serban and V. Pasquier, Phys. Rev. B **67**, 214413 (2003).
- <sup>15</sup> See also paragraph 5.6 of Ref. 2
- <sup>16</sup> R. Moessner, S. L. Sondhi, and E. Fradkin, Phys. Rev. B **65**, 024504 (2002).
- <sup>17</sup> R. Moessner and S. L. Sondhi, Phys. Rev. B **68**, 054405 (2003).
- <sup>18</sup> B. Douçot, M. V. Feigel'man and L. B. Ioffe, Phys. Rev. Lett. **90**, 107003 (2003).
- <sup>19</sup> In fact  $H$  can be any trivalent lattice (each site has three neighbors) with any topology: disk, sphere, cylinder, torus etc... As an example,  $H$  can be an hexagonal lattice with periodic boundary conditions in one direction (cylinder). Then one constructs a new lattice  $K$  by the medial lattice construction: sites of  $K$  are the middle points of the bonds of  $H$ .<sup>14</sup> In the following, for simplicity, we will choose  $H$  to be an hexagonal lattice and  $K$  as a kagome lattice (hence the names  $H$  and  $K$ ).
- <sup>20</sup> In terms of dimers,  $\sigma_h^x$  is the sum of all possible “kinetic energy” terms (ring exchange) which can be defined inside the star surrounding  $h$ . Those terms allow from 3 to 6 dimers to move.
- <sup>21</sup> Those bond variables are  $\mathbb{Z}_2$  gauge degrees of freedom<sup>4</sup> while the local constraint is the Gauss law of the gauge description.<sup>16</sup> As for  $\sigma_h^x = \prod_{i=1}^6 \tau_i^z$ , it is the gauge flux going through the hexagon  $h$ .
- <sup>22</sup> They are independent pseudo-spin operators. Notice however that if the system has no edge (torus or sphere), they are subjected to the an additional constraint  $\prod_h \sigma^x(h) = 1$ . This comes from the fact that, in such a geometry,  $\prod_h \sigma^x(h)$  flips every arrow *twice* and thus reduces to the identity.
- <sup>23</sup> Here local means that the associated loop does not wind around the whole system (cylinder).
- <sup>24</sup> The case where the potential term pins the dimers along some reference configuration in the *whole* system is discussed in Ref. 4 and is equivalent to a 2D Ising model in transverse field.
- <sup>25</sup> These are bonds where the arrows have different orientations in  $c$  and in the reference.
- <sup>26</sup> The relation between the  $\tau$  and  $\sigma$  operators is the same as the standard duality between Ising models and  $\mathbb{Z}_2$  gauge theory in 2+1 dimensions. See Ref. 4
- <sup>27</sup> The relation between topological sectors of QDM and boundary conditions in spin models was already noted in Refs.<sup>4,16,17</sup>, together with the connexion between confinement transition and Ising transition.
- <sup>28</sup> If a monomer winds around the cylinder it connects a configuration  $T^x = 1$  with a configuration  $T^x = -1$ .
- <sup>29</sup> In the  $\mathbb{Z}_2$  gauge theory language the constraint is the Gauss law and allowing triangles with  $\tau_{t_0}^x \tau_{t_1}^x \tau_{t_2}^x = -1$  amounts to allow gauge charges (“matter”) in the system.
- <sup>30</sup>  $U$  needs not have the same value in the bulk and along  $\Delta^*$ . One can also choose  $U = \infty$  in the bulk and  $U < \infty$  along  $\Delta^*$  so that monomers can exist and propagate only along the chain.
- <sup>31</sup> This should be compared with  $\sigma_h^z$  which creates a vison on hexagon  $h$ .
- <sup>32</sup> In the circuit proposed in Ref. 7, the state of the qubit could be measured through a weak Josephson junction connecting the tow edges of the cylinder.
- <sup>33</sup> Since any unitary operation can be performed using  $T^x$  and  $T^z$  sequentially, there is no need to analyze the spectrum with  $\lambda \neq 0$  and  $\mu \neq 0$  simultaneously.
- <sup>34</sup> Eq. A5 will insure that  $\sigma_0^z = c_0^\dagger + c_0$  do not appear in  $d_\omega^\dagger$  so that  $d_\omega^\dagger$  and  $d_\omega$  anticommute with  $\sigma_0^z$ .